



HHS Public Access

Author manuscript

IEEE Trans Ultrason Ferroelectr Freq Control. Author manuscript; available in PMC 2018 October 01.

Published in final edited form as:

IEEE Trans Ultrason Ferroelectr Freq Control. 2017 October ; 64(10): 1420–1428. doi:10.1109/TUFFC.

2017.2718841

Histotripsy Treatment of *S. Aureus* Biofilms on Surgical Mesh Samples under Varying Pulse Durations

Timothy A. Bigelow, Member, IEEE,

Center for Nondestructive Evaluation, Iowa State University, Ames, IA 50011

Clayton L. Thomas,

Center for Nondestructive Evaluation, Iowa State University, Ames, IA 50011

Huaiqing Wu, and

Department of Statistics, Iowa State University, Ames, IA 50011

Kamal MF. Itani

VA Boston Healthcare System, Boston University and Harvard Medical School, West Roxbury, MA 02132

Abstract

Prior studies demonstrated that histotripsy generated by high-intensity tone bursts to excite a bubble cloud adjacent to a medical implant can destroy the bacteria biofilm responsible for the infection. The goal of this study was to treat *S. aureus* biofilms on surgical mesh samples while varying the number of cycles in the tone burst to minimize collateral tissue damage while maximizing therapy effectiveness. *S. aureus* biofilms were grown on 1 cm square surgical mesh samples. The biofilms were then treated *in vitro* using a spherically focused transducer (1.1 MHz, 12.9 cm focal length, 12.7 cm diameter) using either a sham exposure or histotripsy pulses with tone burst durations of 3, 5, or 10 cycles (pulse repetition frequency of 333 Hz, peak compressional pressure of 150 MPa, peak rarefactional pressure of 17 MPa). After treatment, the number of colony forming units (CFUs) on the mesh and the surrounding gel was independently determined. The number of CFUs remaining on the mesh for the sham exposure ($4.8 \pm 0.9 \cdot \log_{10}$) (sample mean \pm sample standard deviation- \log_{10} from 15 observations) was statistically significantly different from the 3-cycle ($1.9 \pm 1.5 \cdot \log_{10}$), 5-cycle ($2.2 \pm 1.1 \cdot \log_{10}$), and 10-cycle exposures ($1.0 \pm 1.5 \cdot \log_{10}$) with an average reduction in the number of CFUs of $3.1 \cdot \log_{10}$. The numbers of CFUs released into the gel for both the sham and exposure groups were the same within a bound of $0.86 \cdot \log_{10}$, but this interval was too large to deduce the fate of the bacteria in the biofilm following the treatment.

Index Terms

Ultrasound Therapy; Histotripsy; biofilm infection

I. Introduction

IN the United States, over a million operations are performed annually to repair abdominal hernias at an estimated cost of over \$2.5 billion [1]. The use of surgical mesh following

hernia repair has become standard practice due to lower recurrence rates and shorter hospital stays. One of the most severe complications following hernia repair is mesh related infections [1–5]. The rate of mesh infections has ranged from less than 1% after laparoscopic ventral incisional hernia repair to over 10% [1, 3–6]. In a review of mesh infection studies [1], 27% to 100% of the infections resulted in mesh removal with an average removal rate of ~70%. In addition to patient suffering, cost, and tissue damage associated with mesh removal, hernia recurrence is a common problem following mesh removal with recurrence rates as high as 100% depending on the surgical procedure [5, 6]. A new mesh cannot be immediately placed upon removing the infected mesh as the local infection will simply spread to the new mesh causing a secondary infection. Instead the infection must be resolved before a new mesh can be placed, complicating the hernia repair [6].

Ultrasound has already shown potential for non-invasively treating biofilms when coupled with traditional antibiotic treatments [7–9] where ultrasound appears to increase drug delivery to *Escherichia coli* (*E. coli*) biofilms. However, in these studies, treatment times were long (~24 to 48 hours), and the treatment was not successful for all types of bacteria. For example, *Pseudomonas aeruginosa* (*P. aeruginosa*) biofilms were not successfully treated by the ultrasound exposures, presumably due to the impermeability and stability of the outer membrane of the bacteria [9]. However, our prior studies showed that both *E. coli* and *P. aeruginosa* biofilms could be successfully destroyed non-invasively by using high-intensity, short duration, ultrasound tone bursts at low duty cycles to mechanically destroy the biofilm structure [10, 11]. This technique, termed cavitation-based histotripsy [12], relies on inertial cavitation to disrupt the biofilm structure. Noninvasive therapies would allow the biofilm to be treated and the infection resolved without needing additional surgeries.

Inertial cavitation, often referred to simply as cavitation, is the dramatic expansion and subsequent collapse of a gas body (i.e., micron-sized bubble or cloud of bubbles) in a fluid medium upon exposure to ultrasound. The collapse of the microbubbles near a solid or tissue boundary results in the formation of a microjet [13, 14], which will mechanically shred the cells or bacteria in the case of a biofilm. When producing inertial cavitation in the MHz frequency range, the mechanical destruction is so fine that it can split a cell in half. Also, in a recent study, 99% of the tissue debris from the cavitation-induced destruction of cells were found to be less than 6 μm in diameter [15] indicating that cavitation-based therapies can be safely used without creating emboli. Inertial cavitation can be generated *in vivo* by positioning the focus of an ultrasound transducer at the desired location and destroying only the targeted cells without damaging the rest of the tissue along the propagation path [15–32]. The bubble cloud responsible for the destruction can be clearly seen in an ultrasound image, allowing for precise therapy control [33, 34].

In our initial study, *E. coli* was grown as a biofilm in chambered microscope slides (4 well Permanox, Lab-Tek Chamber Slide System, Nalge Nunc International, Rochester, NY) as is described in [10]. The biofilms were then exposed to ultrasound at one of six different exposure levels including a sham exposure. A raster scanning pattern with a step size of 750 μm (~ half the beam width) and a delay of 30 seconds between steps was used to treat the entire biofilm. The exposures consisted of 10 cycle tone bursts with a frequency of 1.1 MHz

(pulse duration of $9.1 \mu\text{s}$) at a pulse repetition frequency (PRF) of 1000 Hz (1 ms delay between tone bursts). The peak rarefactional pressure, p_r , for each exposure was varied as 0 (sham), 6 MPa, 7.9 MPa, 10 MPa, 11.9 MPa, and 14.6 MPa, after including the contribution from the reflected wave. After the ultrasound exposure, the number of viable bacteria remaining in the biofilm was determined by dilution plating on media to measure the number of viable bacteria capable of forming a colony [colony forming units, CFUs]. The number of CFUs remaining varies over several orders of magnitude even for identical exposure conditions. However, a statistically significant number of the biofilms at the highest two exposure levels (i.e., p_r of 11.9 and 14.6 MPa) had no viable bacteria. The average number of CFUs in the highest exposure levels was $4.6/\text{mm}^2$ whereas the average number of CFUs in the control was $1.1 \times 10^5/\text{mm}^2$, which is a 4.4-log_{10} reduction of bacteria in the biofilm.

After completing the experiments with the *E. coli* biofilms, *P. aeruginosa* biofilms were grown on Pyrolytic graphite plates [11]. The biofilms were either not exposed (control) or exposed to ultrasound with a peak rarefactional pressure of 13 MPa (larger than pressure threshold necessary for destroying *E. coli* biofilms) utilizing 20-cycle sine wave tone bursts. For the ultrasound exposures, the exposure time at each location on the surface of the biofilm varied from 30 seconds per location (similar to earlier study) to 5 seconds per location while the period between the tone bursts was varied from 1 to 12 ms ($n=6$ repetitions/exposure condition). The entire surface of the graphite was treated by once again moving the focus of the ultrasound transducer in a raster scanning pattern with a step size of $750 \mu\text{m}$ over the whole surface. An epifluorescence microscopy image of the surface of the implant was then used to determine the percent coverage of the plate by live and dead bacteria. From these results, we deduced that the bacteria biofilms were completely destroyed as there was no statistical difference between the sterile plate and the exposed plate at the higher exposure levels. Also, the destruction occurred much faster and with fewer tone bursts than was used in our *E. coli* study (30 s exposure with 1 ms period). Also, increasing the number of tone bursts for the same acoustic pressure increased biofilm destruction (see 15s/3ms exposure versus 5s/3ms exposure).

Our initial work, while promising, focused on treating bacteria biofilms on planar surfaces as these were the simplest geometry on which to grow and expose the biofilms. However, as we move towards the clinical application of surgical mesh infections, we need to verify that our treatment will be equally effective for the mesh geometry. In addition, we need to determine the optimal pulse duration for treating the bacteria biofilms as the level of tissue damage is directly correlated with the duration of the pulse [33, 35, 36]. Lastly, we need to confirm that biofilm destruction can also be achieved for *Staphylococcus aureus* (*S. aureus*) biofilm given its prevalence in mesh infections following hernia repair [1, 3, 5]. Therefore, in this study, *S. aureus* biofilms were grown on surgical mesh samples and exposed in vitro to ultrasound histotripsy pulses with varying pulse duration. The number of CFUs was then used to assess the effectiveness of the therapy for each pulse duration. In addition, the expected collateral damage was separately quantified for each exposure condition using an ultrasound gel pad as a tissue mimic.

II. Methods

A. Biofilm Preparation

Staphylococcus aureus subsp. Aureus (ATCC@25923TM) biofilms were grown on 10 mm × 10 mm samples of Polypropylene mesh (PPKM301, Surgical Mesh Division, Textile Development Associates Inc., Brookfield, CT) as shown in Figure 1.

The biofilms were grown on the mesh by placing each mesh sample in 20 ml of tryptic soy broth (TSB) with one mesh sample per tube. The tubes were then inoculated with 20 μ l of stationary phase bacteria grown over the previous night to initiate biofilm growth. The tubes were then incubated for 24 hours at 37°C. After 24 hours, the mesh was removed using sterile forceps and transferred to a new tube filled with 20 ml of TSB. Inoculation of the second tube was not necessary as the mesh carried sufficient bacteria from one tube to the next. This tube was incubated for 24 hours at 37°C. Afterwards, the mesh was transferred to a new tube with 20 ml of TSB a final time, and incubated again for 24 hours again at 37°C (3 days total). This growth time was determined by varying the time from 1 to 4 days in exploratory studies and determining the number of CFUs on the mesh. The exploratory studies revealed that 3 days of incubation were optimal for our study.

S. aureus was selected for our studies due to its prevalence in mesh infections following hernia repair [1, 3, 5]. PPKM301 was selected from the over 200 meshes on the market [37], as it is a monofilament mesh with relatively large pores (1.5 × 1.2 mm) and small filament diameter (80 μ m). Large pore meshes seem to correlate with better clinical outcome [2, 37], and therefore, we expect them to be the dominant surgical mesh for hernia repair in the future. The large pore size (larger than the focal dimensions) and small filament diameter (smaller than the acoustic wavelength) should also allow for cavitation activity to be generated on all sides of the filaments, improving the efficacy of the proposed treatments.

B. Ultrasound Treatment of the Infected Mesh

After growing the biofilm, the mesh sample was removed from the growth chamber with sterile forceps and gently rinsed with 10ml of sterile phosphate buffered saline (PBS) to remove any planktonic bacteria. The sample was then placed in an Aquaflex Ultrasound Gel Pad Standoffs (Parker Laboratories Inc., Fairfield, NJ) by first cutting the gel pad in half and then cutting a slit into the middle of the gel pad in which the mesh could be inserted. This left approximately 10 mm of gel pad on either side of the mesh. After inserting the mesh, 100 μ l of sterile PBS was also injected into the slit with the mesh. The gel pad with mesh was then placed in a holder in a water bath and exposed to the appropriate ultrasound level. The gel pads were selected as they are bacteriostatic and will thus minimize bacteria growth and have approximately the same mechanical properties as abdominal muscle [38–40]. Mechanical properties have a significant impact on cavitation-histotripsy treatments, such as those used in our study, and therefore it is important they be relatively similar to real biological tissue [33, 41, 42]. The gel pads also provided a consistent material for the exposures.

Once placed into the water bath, the focus of the ultrasound therapy transducer was aligned with the mesh sample by using a low-power signal from a pulser-receiver (Panametrics

5900, Olympus Corporation, Tokyo, Japan) as illustrated in Figure 2. The panametrics excites the transducer with a voltage spike when operating in pulse-echo mode. The therapy transducer was a single-element spherically focused transducer with an operating frequency of 1.1 MHz, a focal length of 12.5 cm, and a diameter of 12.5 cm (H-161C, Sonic Concepts Inc., Bothell, WA). For the alignment, the echo from one of the mesh fibers was first maximized by moving the transducer both in the plane of the mesh and perpendicular to the mesh using a custom computer controlled 3-axis positioning system (BiSlide Assemblies, VELMEX Inc., Bloomfield, NY, USA).

Once aligned on a fiber, the edges of the mesh were identified by observing when the echo from the mesh could no longer be observed while moving the transducer in 1 mm steps in the plane of the mesh. The ultrasound source was driven at a pulse repetition frequency of 2 kHz with a focal pressure amplitude of either 0.076 MPa or 0.15 MPa for the alignment as determined by measurements with our capsule hydrophone (ONDA HGL-0200, Onda Corporation, Sunnyvale, CA, USA). Initially, the lower pressure was used for the alignment; however, alignment was easier at a slightly higher pressure, so the later exposures used the higher amplitude. The pressure pulses used for the alignment are shown in Figure 3.

Once aligned, the mesh sample was randomly exposed to either a sham exposure or histotripsy pulses with tone burst durations of 3, 5, or 10 cycles at a pulse repetition frequency (PRF) of 333 Hz, a peak-compressional pressure of approximately 150 MPa, and a peak rarefactional pressure of approximately 17 MPa. These pressures were determined for our ultrasound therapy transducer using a combination of hydrophone measurements and computer modelling as has been explained in detail in our earlier publications [11, 41, 43, 44]. Each pulse duration including the sham was repeated 15 times. The entire mesh was exposed by scanning the focal point of the transducer in a raster pattern using a step size of 750 μm with an exposure duration of 15 seconds per location. This step size, exposure duration, and PRF were found to be optimal in our earlier histotripsy and biofilm studies [10, 11, 45]. In order to ensure that the entire mesh was treated, the scans were typically 11 to 16 mm on a side as was determined from our alignment procedure for each mesh. The sham exposures were conducted exactly the same as the treatments, including the movement of the transducer, with the only difference being that the therapy source was off for the sham exposures.

C. Assessment of CFUs

Following the treatment, the gel pad with the inserted mesh was removed from the holder. The pad was then cut using a sterile blade so that the top portion of the pad could be lifted away from the mesh sample. This top portion usually corresponded to the portion of the gel pad that was on the far side of the mesh, opposite the transducer. The mesh was then lifted off of the gel pad using sterile forceps and immersed into a tube of 4.5 ml of sterile PBS. This was done to remove any gel fragments on the mesh but not the bacteria still attached to the mesh via biofilm. The mesh was then transferred to a 0.6 ml microcentrifuge tube containing 500 μl of sterile PBS. The gel pad was then scrapped with a sterile blade to remove the surface of the gel that had been in contact with the mesh as well as any gel fragments that had been disrupted by the action of the cavitation. The scrapped gel and

fragments were placed in the same container in which the mesh was immersed upon its removal from the gel. This allowed for the determination of the number of CFUs released into the gel as well as the number of CFUs remaining on the mesh for every exposure.

The 0.6 ml microcentrifuge tube containing the mesh was then vortexed for 60 seconds. It was placed in a Symphony Ultrasonic Cleaner (1.9 L, VWR, Radnor, PA) and sonicated for two minutes. It was then vortexed for 60 seconds, sonicated for two minutes, and vortexed again for 60 seconds. This process broke apart the biofilm without killing the bacteria. Following the sonication and vortexing, 500 μ l was removed and serially diluted in sterile PBS to the following dilutions: 10^{-1} , 10^{-2} , 10^{-3} , 10^{-4} , and 10^{-5} . The tube with the gel fragments was vortexed for three minutes and diluted likewise. 100 μ l of each dilution was plated on tryptic soy agar and grown overnight at 37° C. CFUs were counted the next day. These data were used to back calculate the total number of CFUs both remaining on the mesh and present in the disrupted gel after histotripsy. The number of CFUs reported corresponded to the dilution that had between 30 and 300 for each case as counts in this range have been shown to be the most reliable. If two different dilutions had counts in this range, the numbers were averaged after accounting for the dilution process. If all of the counts were outside the 30–300 range, then the count from the dilution that was closest to 300 was used. Lastly, if the plate counts were zero for the lowest dilution, the count was set to zero. Once the number of CFUs was determined for either the mesh or the gel, the goal was to determine the \log_{10} -reduction in the number of CFUs between the sham and each exposure condition. Therefore, we calculated $\log_{10}(\text{count}+1)$ to translate the count into log number for comparison. This transformation avoided the problem with $\log_{10}(\text{count})$ when the count is zero, and also allowed the transformed data for each of the four groups to follow a normal distribution simplifying the statistical analysis of the data [46].

D. Statistical Analysis

We analyzed the transformed data for the mesh using one-way analysis of variance (ANOVA) and JMP software (Pro 12, The SAS Institute). The data included 60 observations, 15 for each of the sham and three exposure groups. The Tukey-Kramer honest significant difference (HSD) method (with an overall type I error rate of no more than 5%) was used for pairwise comparisons between the four groups. The HSD also gave 95% simultaneous confidence intervals for all pairwise differences. We then used the same method to analyze the transformed data for the gel (again with 15 observations per group). One of the 10-cycle exposure cases had 4.8- \log_{10} CFUs for the mesh, an order of magnitude more than any of the other exposures, including the lower energy exposures of 3 and 5 cycles. To see how this observation affected our analysis results, we used one-way ANOVA and the HSD to analyze the other 59 observations. The plot of residuals versus predicted values and the normal probability plot of the residuals indicate that the model in all three cases is adequate.

E. Ultrasound Treatments for Collateral Damage Assessment

In addition to assessing each treatment in terms of efficacy, we also quantified the damage done to the gel near the mesh. These measurements were done independently of the biofilm treatments as both the variability in treatment dimensions and the variability in scraping the

gel would impact our results. Therefore, for these measurements, mesh samples without biofilms were placed in the gel pads as had been done previously. However, since cross contamination was not a concern and the gel pads were relatively large relative to the mesh samples, two mesh samples were placed in each gel pad. The focus of the ultrasound therapy transducer was then aligned with each mesh sample, and a square raster scan was performed with dimensions of 5.25 mm on a side with a step-size of 750 μm for tone bursts of 3, 5, and 10 cycles. The sham exposure was not included as no damage was observed for the sham exposures in any of the biofilm treatments. The scans were centered at the middle of the gel pads based on the alignment exposures. Since the mesh samples were 10 mm \times 10 mm, using a scan smaller than the mesh avoided any edge effects.

Following the treatments, the gel pads were cut to isolate the mesh samples. The meshes were then removed and the gel pads were rinsed to remove any debris similar to our earlier work [33, 41–43, 45]. This left relatively square holes in the mesh samples. The lateral dimensions of the holes were measured by calipers while the volume was measured by filling each hole with water until it overflowed similar to our earlier studies. The experiment was repeated 5 times for each exposure condition.

III. Results

A. Bacteria Viability

The results for the number of CFUs remaining on the mesh for each of the treatment settings are shown in Figure 4.

The number of CFUs remaining on the mesh for the sham exposure was $4.8 \pm 0.9 \cdot \log_{10}$ (sample mean \pm sample standard deviation- \log_{10} of 15 observations) which was statistically significantly different from the 3-cycle ($1.9 \pm 1.5 \cdot \log_{10}$), 5-cycle ($2.2 \pm 1.1 \cdot \log_{10}$), and 10-cycle exposures ($0.97 \pm 1.5 \cdot \log_{10}$) with an average reduction in the number of CFUs of $3.1 \cdot \log_{10}$. None of the treated exposures were statistically different from each other due to the large variability in the results.

The numbers of CFUs released onto the gel for the sham and exposure cases are shown in Figure 5. These numbers are the same within a bound of $0.86 \cdot \log_{10}$; that is, Tukey's 95% simultaneous confidence interval for each pairwise difference was contained within $(-0.86, 0.86)$. However, even if all of the bacteria on the mesh were to be released into the gel, this would only increase the number of CFUs by $0.54 \cdot \log_{10}$ based on the sham results due to the large number of CFUs on the gel relative to the mesh. Therefore, we cannot conclusively claim that the number of CFUs on the gel is not increased by the exposures. Hence, we may be releasing the bacteria from the biofilm without killing them.

B. Assessment of Gel Damage

An example of the hole left in the gel following the exposures and rinsing to remove debris is shown in Figure 6.

The hole is relatively square with pits visible in a regular pattern along the bottom. The volume of the holes left in the mesh following the exposures is shown in Figure 7.

These volumes represent only the destruction of the gel structure for the portion of the gel pad in front of the mesh (between the mesh and the transducer) as none of the samples had any perceivable damage behind the mesh. There is a clear and statistically significant increase in lesion volume with increasing acoustic cycles in the tone burst. This increase in lesion volume directly corresponds to an increase in volume depth as the lateral dimensions of the lesion do not change significantly with pulse duration as is shown in Figure 8.

These results agree with prior studies on the dependence histotripsy lesion dimension on tone burst duration [33, 35, 36].

IV. Discussion

In this study, we successfully achieved a reduction of the number of CFUs in our *S. aureus* biofilms by three orders of magnitude (3.1-log_{10}). As a comparison, the FDA definition of high-level disinfection is a reduction in CFUs by 6 orders of magnitude (6-log_{10}). However, achieving this level of disinfection is very difficult even *ex vivo*. For example, an initial cleaning of endoscopes typically only yields a 4-log_{10} reduction in the number of CFUs with a 6-log_{10} reduction only being achieved after an additional soaking in high-level disinfectant for ~20 minutes [47, 48]. *Ex vivo* directed energy methods such as microwave also typically exhibit a 3-log_{10} to 4-log_{10} reduction in CFUs with some tests only showing a reduction of only 2-log_{10} and others achieving the desired 6-log_{10} reduction [49–51]. Therefore, our technique of using ultrasound histotripsy continues to show promise even though we have not yet consistently achieved the 4-log_{10} reduction that was observed in our earlier studies. However, partial treatment of the biofilm is concerning as it could exasperate the problem *in vivo*. Therefore, additional *in vitro* studies are needed to find more effective exposure parameters.

When assessing the data from the CFUs surviving on the mesh, there was some concern over the number of CFUs counted for one of the 10-cycle exposures which had 4.8-log_{10} CFUs. This was an order of magnitude more than any of the other exposures including the lower energy exposures of 3 and 5 cycle. While we are not aware of any reason to reject this data point, its large difference from the other cases is suspicious given the small possibility of contamination or even misalignment in the experiments. If this outlier is excluded from the analysis, the number of CFUs for the 10-cycle exposures is $0.7\pm 1.2\text{-log}_{10}$ which is significantly different from the 3 and 5-cycle exposures. Therefore, the 10-cycle exposures might be better than the other exposures at reducing the number of CFUs on the mesh. However, it is associated with the potential for much more collateral damage.

We may be able to enhance the destruction of the biofilm by using a smaller step size to ensure that all fibers of the mesh are adequately treated. We noticed that when aligning the focus of the ultrasound transducer on the mesh, it was easier to exactly target the mesh fibers when moving with a finer step size as was evidenced by larger amplitudes on the pulse/echo signal. Therefore, reducing the step size may ensure that every fiber is directly targeted. Smaller step sizes, however, will lengthen the treatment time provided the exposure time at each location remains the same. This is why we used the $750\ \mu\text{m}$ steps for this study. Our prior work on ultrasound histotripsy treatment varied the step size when performing

generalized tissue destruction [45], but a similar study has not been conducted for the treatment of bacteria biofilms. However, smaller step sizes may allow for fewer therapy bursts (i.e., shorter exposure time) at each treatment location as has been shown in other studies [44, 45]. A smaller step size may also reduce the variability in our mesh treatments (Figure 4) as the location of the individual mesh fibers relative to the beam profile may have resulted in varying levels of exposure effectiveness.

One limitation of our study is that we were not able to ascertain the fate of bacteria released from the biofilm as the result of our exposure. The sham and treatment exposures did not have a statistically different number of bacteria on the gel, but the confidence interval was too large to claim that they were the same. Hence, we may be releasing the bacteria from the biofilm without killing them. This possibility is doubtful given the fragmentation of microalgae that was observed in some of our earlier studies [52, 53], but we cannot make the claim of bacteria killing from this study. Instead, all we can conclusively say is that the biofilms have been disrupted by our therapy while our hypothesis continues to be that the bacteria are destroyed and not just released. Testing of this hypothesis in our present study was confounded by the large number of bacteria spontaneously released from the biofilm, even for the sham exposures. On average, only 34% of the total number of CFUs (mesh+gel) remained on the mesh following the sham treatments. Given that released bacteria could easily migrate from an untreated region to a region where the histotripsy treatment has already been completed without crossing the current treatment zone means that many of the bacteria on the gel could have been completely missed by the ultrasound exposures.

As we look forward to moving towards clinical implementation, the two most critical aspects are improving the effectiveness of biofilm destruction on the mesh and reducing the required treatment time. The treatment of 1 cm² of mesh takes about 50 minutes. Therefore, the 150 cm² meshes used clinically would take ~125 hours doing a basic raster scan. One solution that has been implemented in histotripsy applications is to use an array transducer which sends a therapy pulse to different spatial regions rather than turning the source off between the tone bursts. Given that the duty cycle is on the order of 0.1% this could theoretically result the therapy being performed 1000x faster. In practice, the improvement is not as dramatic due to heating concerns of the intervening tissue layers.

V. Conclusion

In this study, we successfully demonstrated an average reduction of 3.1- \log_{10} in the number of CFUs for *S. aureus* biofilms grown on mesh samples. The largest reduction was achieved for the 10-cycle tone burst exposures with a reduction of 3.8- \log_{10} . However, this reduction was not statistically significantly different from the 3-cycle tone burst exposures, and the 10-cycle exposures resulted in approximately six times as much collateral damage to our tissue mimic. Therefore, the 3-cycle tone burst is probably the best treatment option moving forward. Even if the 10-cycle exposures were statistically significantly better, there may be other ways to make-up the 1- \log_{10} reduction in CFUs while achieving less collateral tissue damage. There was not a statistically significant change in the number of CFUs on the gel following the ultrasound exposures with the variability in the CFUs and the large number of

bacteria released into gel making it difficult to determine if the bacteria were killed or released when the biofilm was destroyed.

Acknowledgments

This research was supported by National Institutes of Health (NIH) grant number R21EB020722.

References

1. Mavros M, Athanasiou S, Alexiou V, Mitsikostas P, Peppas G, Falagas M. Risk Factors for Mesh-related Infections After Hernia Repair Surgery: A Meta-analysis of Cohort Studies. *World Journal of Surgery*. 2011; 35:2389–2398. [PubMed: 21913136]
2. Amid P. Classification of biomaterials and their related complications in abdominal wall hernia surgery. *Hernia*. 1997; 1:15–21.
3. Falagas ME, Kasiakou SK. Mesh-related infections after hernia repair surgery. *Clinical Microbiology and Infection*. 2005; 11:3–8.
4. Lüning T, Spillenaar-Bilgen EJ. Parastomal hernia: complications of extra-peritoneal onlay mesh placement. *Hernia*. 2009; 13:487–490. [PubMed: 19322626]
5. Sanchez VM, Abi-Haidar YE, Itani KMF. Mesh infection in ventral incisional hernia repair: Incidence, contributing factors, and treatment. *Surgical Infections*. 2011; 12:205–210. [PubMed: 21767146]
6. LeBlanc KA. Laparoscopic incisional and ventral hernia repair: Complications—how to avoid and handle. *Hernia*. 2004; 8:323–331. [PubMed: 15235939]
7. Rediske AM, Roeder BL, Nelson JL, Robison RL, Schaalje GB, Robison RA, et al. Pulsed Ultrasound Enhances the Killing of *Escherichia coli* Biofilms by Aminoglycoside Antibiotics In Vivo. *Antimicrob Agents Chemother*. Mar.2000 44:771–772. [PubMed: 10681355]
8. Qian Z, Sagers RD, Pitt WG. Investigation of the mechanism of the bioacoustic effect. *Journal of Biomedical Materials Research*. 1999; 44:198–205. [PubMed: 10397921]
9. Carmen JC, Roeder BL, Nelson JL, Robison Ogilvie RL, Robison RA, Schaalje GB, et al. Treatment of biofilm infections on implants with low-frequency ultrasound and antibiotics. *American Journal of Infection Control*. 2005; 33:78–82. [PubMed: 15761406]
10. Bigelow TA, Northagen T, Hill TM, Sailer FC. The Destruction of *Escherichia Coli* Biofilms Using High-Intensity Focused Ultrasound. *Ultrasound in Medicine & Biology*. 2009; 35:1026–1031. [PubMed: 19171416]
11. Xu J, Bigelow TA, Halverson LJ, Middendorf JM, Rusk B. Minimization of treatment time for in vitro 1.1 MHz destruction of *Pseudomonas aeruginosa* biofilms by high-intensity focused ultrasound. *Ultrasonics*. 2012; 52:668–675. [PubMed: 22341761]
12. Khokhlova VA, Fowlkes JB, Roberts WW, Schade GR, Xu Z, Khokhlova TD, et al. Histotripsy methods in mechanical disintegration of tissue: Towards clinical applications. *International Journal of Hyperthermia*. Feb 17.2015 31:145–162. [PubMed: 25707817]
13. Gracewski SM, Miao H, Dalecki D. Ultrasonic excitation of a bubble near a rigid or deformable sphere: Implications for ultrasonically induced hemolysis. *The Journal of the Acoustical Society of America*. 2005; 117:1440–1447. [PubMed: 15807031]
14. Brujan EA. The role of cavitation microjets in the therapeutic applications of ultrasound. *Ultrasound in Medicine & Biology*. 2004; 30:381–387. [PubMed: 15063520]
15. Xu Z, Fan Z, Hall TL, Winterroth F, Fowlkes JB, Cain CA. Size Measurement of Tissue Debris Particles Generated from Pulsed Ultrasound Cavitation Therapy - Histotripsy. *Ultrasound in Medicine & Biology*. 2009; 35:245–255. [PubMed: 19027218]
16. Cain, C. Histotripsy: Controlled mechanical sub-division of soft tissues by high intensity pulsed ultrasound. 5th International Symposium on Therapeutic Ultrasound; Boston, MA. 2005. p. T005
17. Hall TL, Fowlkes B, Cain CA. A real-time measure of cavitation induced tissue disruption by ultrasound imaging backscatter reduction. *Ultrasonics, Ferroelectrics and Frequency Control, IEEE Transactions on*. 2007; 54:569–575.

18. Hall, TL., Fowlkes, JB., Cain, CA. Imaging feedback of tissue liquefaction (histotripsy) in ultrasound surgery. 2005 IEEE Ultrasonics Symposium; 2005. p. 1732-1734.
19. Maxwell AD, Cain CA, Duryea AP, Yuan L, Gurm HS, Xu Z. Noninvasive Thrombolysis Using Pulsed Ultrasound Cavitation Therapy - Histotripsy. *Ultrasound in Medicine & Biology*. 2009; 35:1982–1994. [PubMed: 19854563]
20. Maxwell, AD., Cain, CA., Gurm, HS., Fowlkes, JB., Zhen, X. Non-invasive thrombolysis induced by histotripsy pulsed cavitation ultrasound therapy. *Ultrasonics Symposium, 2008. IUS 2008; IEEE; 2008. p. 1167-1170.*
21. Maxwell, AD., Owens, G., Gurm, HS., Cain, CA., Xu, Z. In-vivo study of non-invasive thrombolysis by histotripsy in a porcine model. *Ultrasonics Symposium (IUS), 2009 IEEE International; 2009. p. 220-223.*
22. Maxwell, AD., Tzu-Yin, W., Cain, CA., Fowlkes, JB., Xu, Z., Sapozhnikov, OA., et al. The role of compressional pressure in the formation of dense bubble clouds in histotripsy. *Ultrasonics Symposium (IUS), 2009 IEEE International; 2009. p. 81-84.*
23. Parsons JE, Cain CA, Fowlkes JB. Spatial variability in acoustic backscatter as an indicator of tissue homogenate production in pulsed cavitation ultrasound therapy. *Ultrasonics, Ferroelectrics and Frequency Control, IEEE Transactions on*. 2007; 54:576–590.
24. Roberts, WW., Hall, TL., Hempel, CR., Cain, CA. Prostate histotripsy for BPH: initial canine results. *Photonic Therapeutics and Diagnostics V; San Jose, CA, USA. 2009. p. 71611N-8*
25. Wang, T-y, Xu, Z., Winterroth, F., Hall, TL., Fowlkes, JB., Rothman, ED., et al. Quantitative ultrasound backscatter for pulsed cavitation ultrasound therapy-histotripsy. *Ultrasonics, Ferroelectrics and Frequency Control, IEEE Transactions on*. 2009; 56:995–1005.
26. Xu Z, Raghavan M, Hall TL, Ching-Wei C, Mycek MA, Fowlkes JB, et al. High Speed Imaging of Bubble Clouds Generated in Pulsed Ultrasound Cavitation Therapy - Histotripsy. *Ultrasonics, Ferroelectrics and Frequency Control, IEEE Transactions on*. 2007; 54:2091–2101.
27. Xu Z, Raghavan M, Hall TL, Mycek MA, Fowlkes JB, Cain CA. Evolution of Bubble Clouds Induced by Pulsed Cavitation Ultrasound Therapy-Histotripsy. *Ultrasonics, Ferroelectrics and Frequency Control, IEEE Transactions on*. 2008; 55:1122–1132.
28. Kim, Y., Fifer, CG., Gelehrter, SK., Williams, J., Lu, JC., Cain, CA., et al. Non-invasive fetal therapy using histotripsy: Feasibility study in the sheep model. *Ultrasonics Symposium (IUS), 2009 IEEE International; 2009. p. 228-231.*
29. Xu Z, Fowlkes JB, Cain CA. A new strategy to enhance cavitation tissue erosion using a high-intensity, initiating sequence. *Ultrasonics, Ferroelectrics and Frequency Control, IEEE Transactions on*. 2006; 53:1412–1424.
30. Xu Z, Fowlkes JB, Ludomirsky A, Cain CA. Investigation of intensity thresholds for ultrasound tissue erosion. *Ultrasound in Medicine & Biology*. 2005; 31:1673–1682. [PubMed: 16344129]
31. Xu Z, Fowlkes JB, Rothman ED, Levin AM, Cain CA. Controlled ultrasound tissue erosion: The role of dynamic interaction between insonation and microbubble activity. *The Journal of the Acoustical Society of America*. 2005; 117:424–435. [PubMed: 15704435]
32. Xu Z, Ludomirsky A, Eun LY, Hall TL, Tran BC, Fowlkes JB, et al. Controlled ultrasound tissue erosion. *Ultrasonics, Ferroelectrics and Frequency Control, IEEE Transactions on*. 2004; 51:726–736.
33. Xu J, Bigelow TA, Nagaraju R. Precision control of lesions by high-intensity focused ultrasound cavitation-based histotripsy through varying pulse duration. *Ultrasonics, Ferroelectrics and Frequency Control, IEEE Transactions on*. 2013; 60
34. Vlasisavljevich E, Kim Y, Allen S, Owens G, Pelletier S, Cain C, et al. Image-Guided Non-Invasive Ultrasound Liver Ablation Using Histotripsy: Feasibility Study in an In Vivo Porcine Model. *Ultrasound in Medicine & Biology*. 2013; 39:1398–1409. [PubMed: 23683406]
35. Xi Z, Owens GE, Gurm HS, Yu D, Cain CA, Zhen X. Noninvasive thrombolysis using histotripsy beyond the intrinsic threshold (microtripsy). *Ultrasonics, Ferroelectrics, and Frequency Control, IEEE Transactions on*. 2015; 62:1342–1355.
36. Kuang-Wei L, Yohan K, Maxwell AD, Tzu-Yin W, Hall TL, Zhen X, et al. Histotripsy beyond the intrinsic cavitation threshold using very short ultrasound pulses: microtripsy. *Ultrasonics, Ferroelectrics and Frequency Control, IEEE Transactions on*. 2014; 61:251–265.

37. Klosterhalfen B, Klinge U. Retrieval study at 623 human mesh explants made of polypropylene – impact of mesh class and indication for mesh removal on tissue reaction. *Journal of Biomedical Materials Research Part B: Applied Biomaterials*. 2013 pp. n/a-n/a.
38. Dogan F, Celebi MS. Quasi-non-linear deformation modeling of a human liver based on artificial and experimental data. *The International Journal of Medical Robotics and Computer Assisted Surgery*. 2015 pp. n/a-n/a.
39. Brown SHM, Carr JA, Ward SR, Lieber RL. Passive Mechanical Properties of Rat Abdominal Wall Muscles Suggest an Important Role of the Extracellular Connective Tissue Matrix. *Journal of Orthopaedic Research*. Jan 20.2012 30:1321–1326. [PubMed: 22267257]
40. Ogneva IV, Lebedev DV, Shenkman BS. Transversal Stiffness and Young's Modulus of Single Fibers from Rat Soleus Muscle Probed by Atomic Force Microscopy. *Biophysical Journal*. 2010; 98:418–424. [PubMed: 20141755]
41. Xu J, Bigelow TA. Experimental Investigation of the Effect of Stiffness, Exposure Time and Scan Direction on the Dimension of Ultrasound Histotripsy Lesions. *Ultrasound in Medicine & Biology*. 2011; 37:1865–1873. [PubMed: 21963031]
42. Xu J, Bigelow TA, Davis G, Avendano A, Shrotriya P, Bergler K, et al. Dependence of ablative ability of high-intensity focused ultrasound cavitation-based histotripsy on mechanical properties of agar. *The Journal of the Acoustical Society of America*. 2014; 136:3018–3027. [PubMed: 25480051]
43. Xu J, Bigelow TA, Riesberg GM. Impact of Preconditioning Pulse on Lesion Formation During High-Intensity Focused Ultrasound Histotripsy. *Ultrasound in Medicine & Biology*. 2012; 38:1918–1929. [PubMed: 22929656]
44. Xu J, Bigelow TA, Whitley EM. Assessment of Ultrasound Histotripsy–Induced Damage to Ex Vivo Porcine Muscle. *Journal of Ultrasound in Medicine*. Jan 1.2013 32:69–82. [PubMed: 23269712]
45. Xu J, Bigelow TA, Lee H. Effect of pulse repetition frequency and scan step size on the dimensions of the lesions formed in agar by HIFU histotripsy. *Ultrasonics*. Apr.2013 53:889–896. [PubMed: 23339995]
46. Olsen CH. Review of the Use of Statistics in Infection and Immunity. *Infection and Immunity*. 2003; 71:6689–6692. [PubMed: 14638751]
47. Rutala W, Weber D. Reprocessing endoscopes: United States perspective. *J Hosp Infect*. 2004; 56:S27–39. [PubMed: 15110120]
48. Rutala WA, Weber DJ. FDA Labeling Requirements for Disinfection of Endoscopes: A Counterpoint. *Infection Control and Hospital Epidemiology*. 1995; 16:231–235. [PubMed: 7636171]
49. Liu Q, Zhang M, Fang Z-x, Rong X-h. Effects of ZnO nanoparticles and microwave heating on the sterilization and product quality of vacuum-packaged Caixin. *Journal of the Science of Food and Agriculture*. 2014 pp. n/a-n/a.
50. Sesma N, Rocha AL, Lagana DC, Costa B, Morimoto S. Effectiveness of Denture Cleanser Associated With Microwave Disinfection and Brushing of Complete Dentures: In Vivo Study. *Brazilian Dental Journal*. 2013; 24:357–361. [PubMed: 24173256]
51. Silva MM, Mima EGdO, Colombo AL, Sanitá PV, Jorge JH, Massucato EMS, et al. Comparison of denture microwave disinfection and conventional antifungal therapy in the treatment of denture stomatitis: a randomized clinical study. *Oral Surgery, Oral Medicine, Oral Pathology and Oral Radiology*. Oct.2012 114:469–479.
52. Bigelow TA, Xu J, Stessman DJ, Yao L, Spalding MH, Wang T. Lysis of *Chlamydomonas reinhardtii* by high-intensity focused ultrasound as a function of exposure time. *Ultrasonics Sonochemistry*. 2014; 21:1258–1264. [PubMed: 24355286]
53. Riesberg G, Bigelow TA, Stessman DJ, Spalding MH, Yao L, Wang T, et al. Flow rate and duty cycle effects in lysis of *Chlamydomonas reinhardtii* using high-energy pulsed focused ultrasound. *The Journal of the Acoustical Society of America*. 2014; 135:3632–3638. [PubMed: 24916410]

Biographies



Timothy A. Bigelow is an Associate Professor with a joint appointment in Electrical/Computer Engineering and Mechanical Engineering at Iowa State University. He was born in Colorado Springs, Colorado in 1976. His research interests focus on improving the diagnostic and therapeutic effectiveness of medical ultrasound. Specifically, he focuses on quantifying the physical properties of tissue for diagnostic purposes using backscattered ultrasound signals, applying ultrasound induced cavitation to destroy unwanted cells, and exploring new ultrasound induced biological effects for both ultrasound safety and ultrasound therapy applications. Dr. Bigelow graduated from the University of Illinois-Urbana in May 2004 with a Ph.D. in Electrical Engineering. After completing his education, he was a Visiting Assistant Professor in the Electrical and Computer Engineering Department at the University of Illinois at Urbana-Champaign for a year. Dr. Bigelow was then an Assistant Professor in Electrical Engineering at the University of North Dakota for three years prior to coming to Iowa State University in August 2008. He was promoted to Associate Professor with Tenure in July 2014 and is currently a Fellow of the American Institute of Ultrasound in Medicine. He currently serves as an Associate Editor for IEEE Ultrasonics, Ferroelectrics, and Frequency Control and is on the Editorial Board of Ultrasonic Imaging.



Clayton L. Thomas was born May 2nd, 1985 in South Bend, Indiana. He attended Purdue University in West Lafayette, Indiana and graduated with a Bachelor of Science in Biology in 2007. Later that year, he began working in WIL Research LLC., a contract research organization in Ashland, Ohio as a biologist in the necropsy department. After two years, he accepted a position as a laboratory manager for Dr. Shaun Lee at the University of Notre Dame in Notre Dame, Indiana. There, he gained valuable experience in the area of microbiology and authored and co-authored several peer-reviewed articles. In 2016, Clayton moved to Iowa to work as a laboratory technician under Dr. Tim Bigelow at Iowa State University in Ames. He is currently at this position conducting research on the effects of histotripsy on bacterial biofilms.



Huaiqing Wu received the B.S. degree in Mathematics in 1988 and the M.S. degree in Statistics in 1991 from Peking University, Beijing, China, and received the Ph.D. degree in Statistics in 1997 from the University of Michigan, Ann Arbor, MI. He then joined the Department of Statistics at Iowa State University as an Assistant Professor of Statistics and has been an Associate Professor of Statistics since 2003. His research interests include experimental design, reliability, engineering statistics, and statistical applications. He received the 2003 Jack Youden Prize for Best Expository Paper in the 2002 volume of *Technometrics*.



Kamal M. F. Itani, MD was born in Beirut Lebanon, obtained his bachelor degree in science with a major in biology and chemistry in 1981 and his Medical degree in 1985 both from the American University of Beirut in Lebanon. He subsequently did a research fellowship in gastrointestinal physiology and motility in the Department of Surgery at Duke University from 1985–1988 followed by a residency in general surgery at Baylor College of Medicine and a clinical fellowship in gastrointestinal surgery from 1988–1994. From 1994–2004, Dr Itani was on the faculty at the Michael E. DeBakey Department of Surgery at Baylor College of Medicine in Houston. From 2000–2004, Dr Itani was also the assistant dean for Graduate Medical Education at Baylor and Chief of General Surgery at the Houston VA Medical Center. From 2004 and to the present time, Dr Itani is the Chief of surgical service at the VA Boston Health Care System, a Professor of Surgery at Boston University, faculty member at Harvard Medical School and the Associate Chief of Surgery at Boston Medical Center and The Brigham and Women’s Hospital.

Dr Itani is a member of various surgical organizations and has served in various leadership positions in these organizations. He is currently the President of The Surgical Infection Society, Chair of the research Committee of the American College of Surgeons and is past President of The Association of VA Surgeons. He sits on the editorial board of the American Journal of Surgery, Surgical Infection, JAMA surgery, and is a reviewer for several medical and surgical journals.

Dr. Itani is the recipient of many awards, including a presidential citation from the Association of VA surgeons in 2016, World Lebanese cultural union 2011 award, a senate proclamation in his name in 2011 and several teaching awards over the years. He was elected as a top doctor by US news and world report and a Castle Connolly top doctor for 5 years in a row.

Author Manuscript

Author Manuscript

Author Manuscript

Author Manuscript

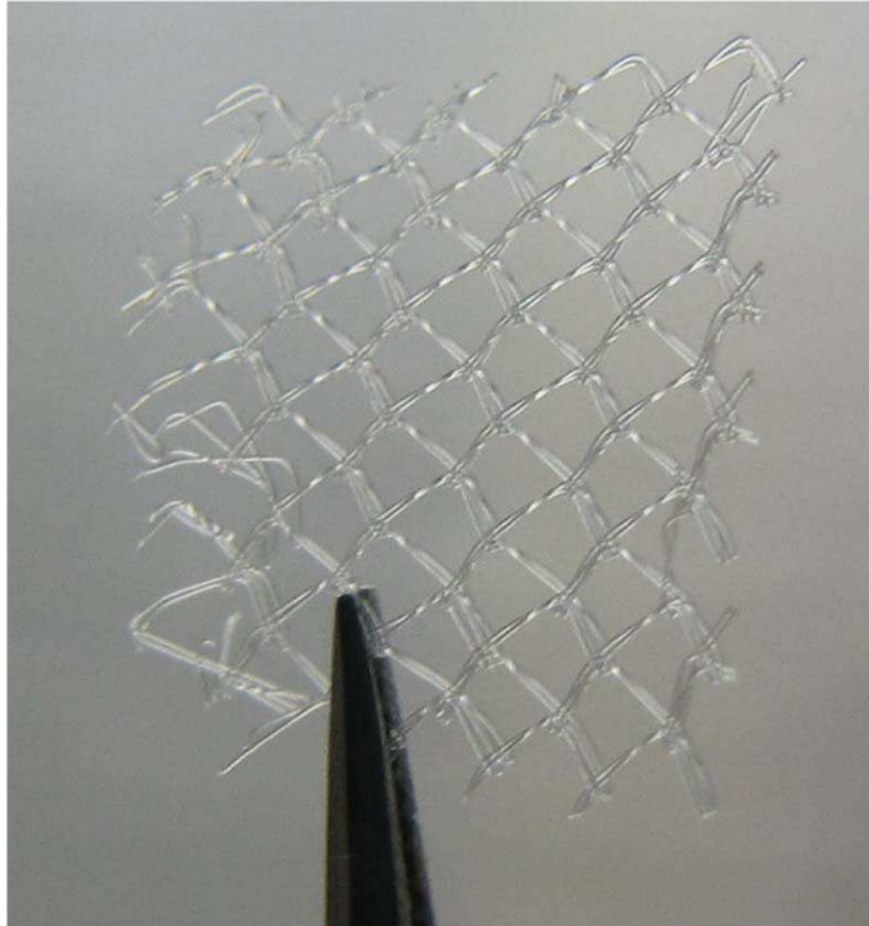


Fig. 1.
Image of Polypropylene mesh sample used in the experiments.

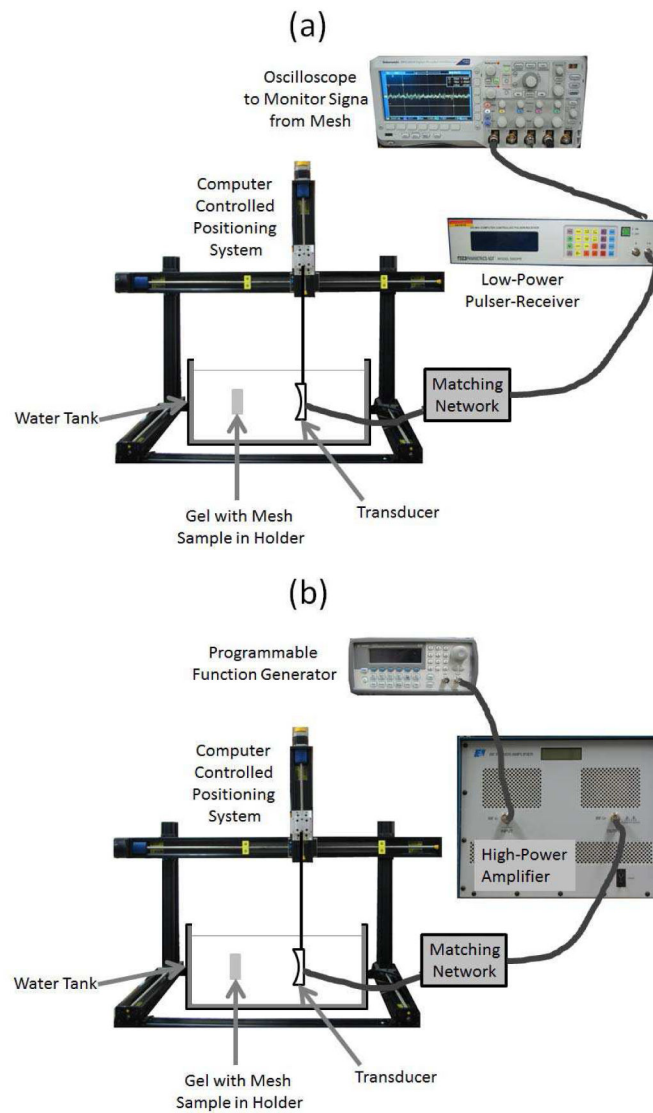


Fig. 2. The experimental set-up utilized when (a) aligning the focus of the ultrasound transducer on the mesh sample, and (b) exposing the the mesh samples to the high-intensity tone bursts.

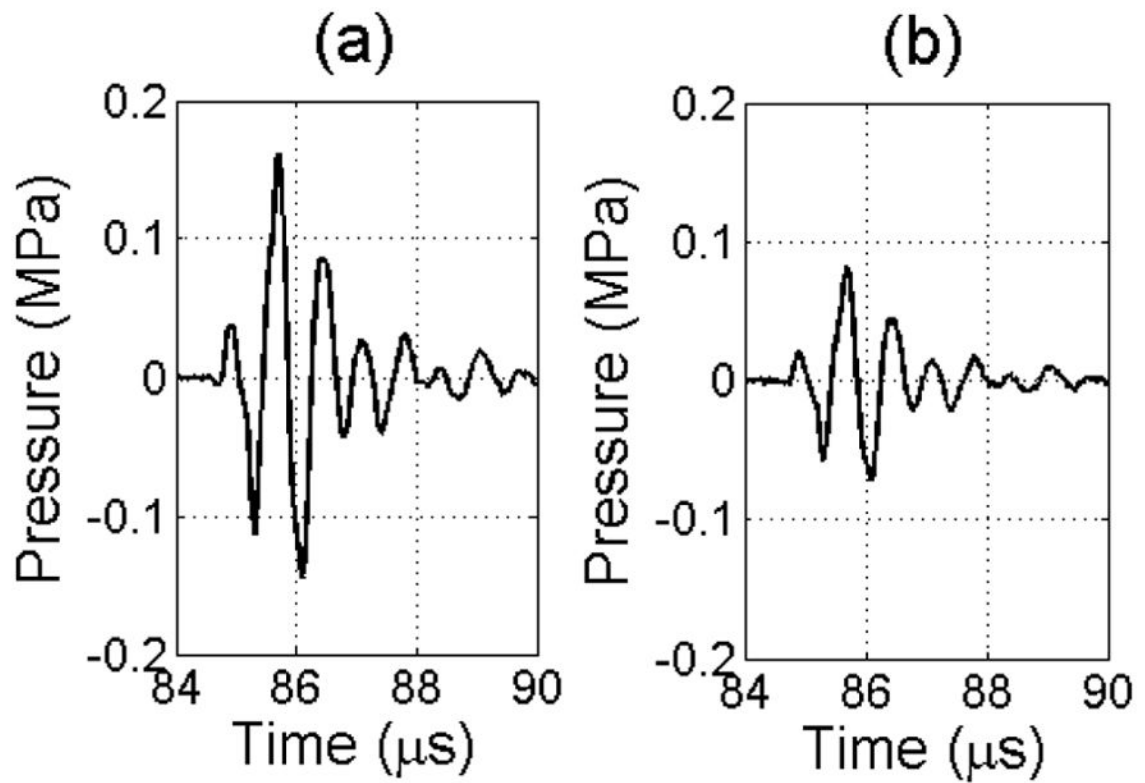


Fig. 3. Pulses used to align the focus of the therapy transducer on the mesh corresponding to a (a) 4 μJ and (b) 2 μJ excitation voltage spike from the Panametrics 5900.

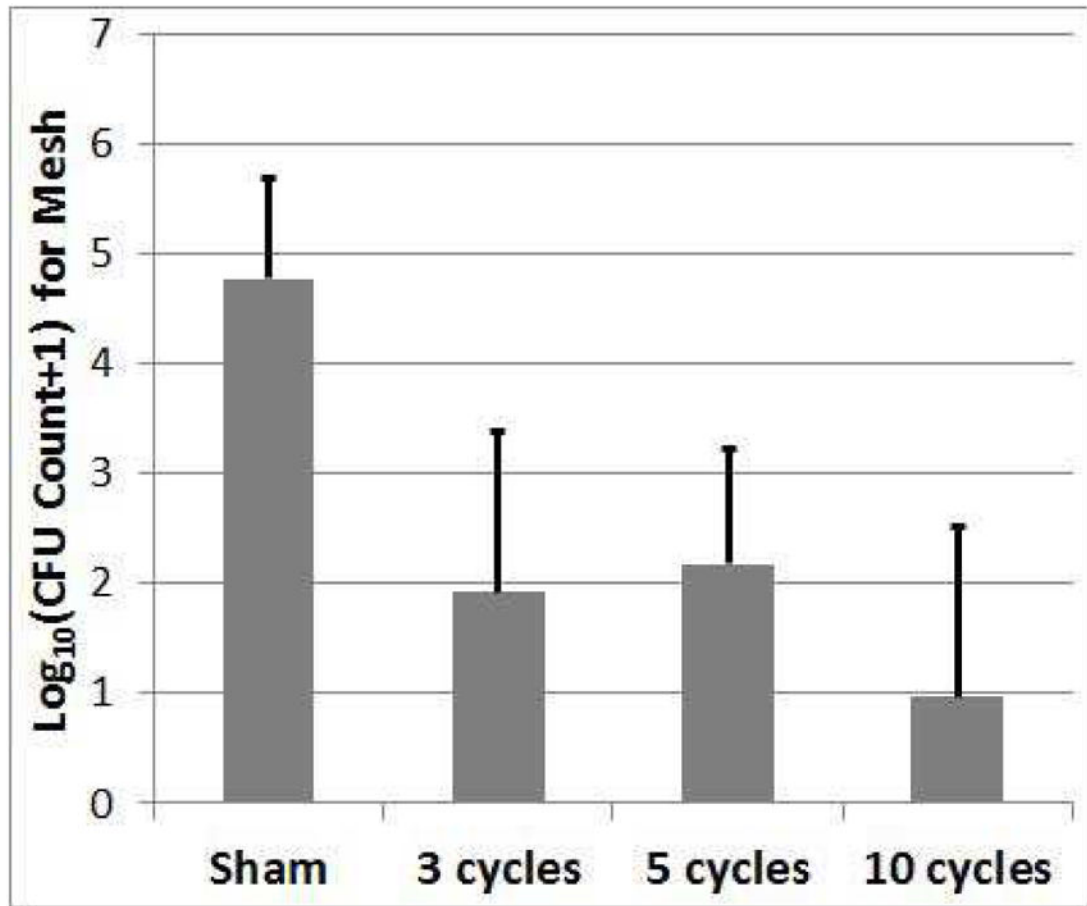


Fig. 4. Count of CFUs surviving on the mesh sample following the treatment as a function of the number of cycles in the tone burst used to treat the biofilm on the mesh. The error bars correspond to one standard deviation.

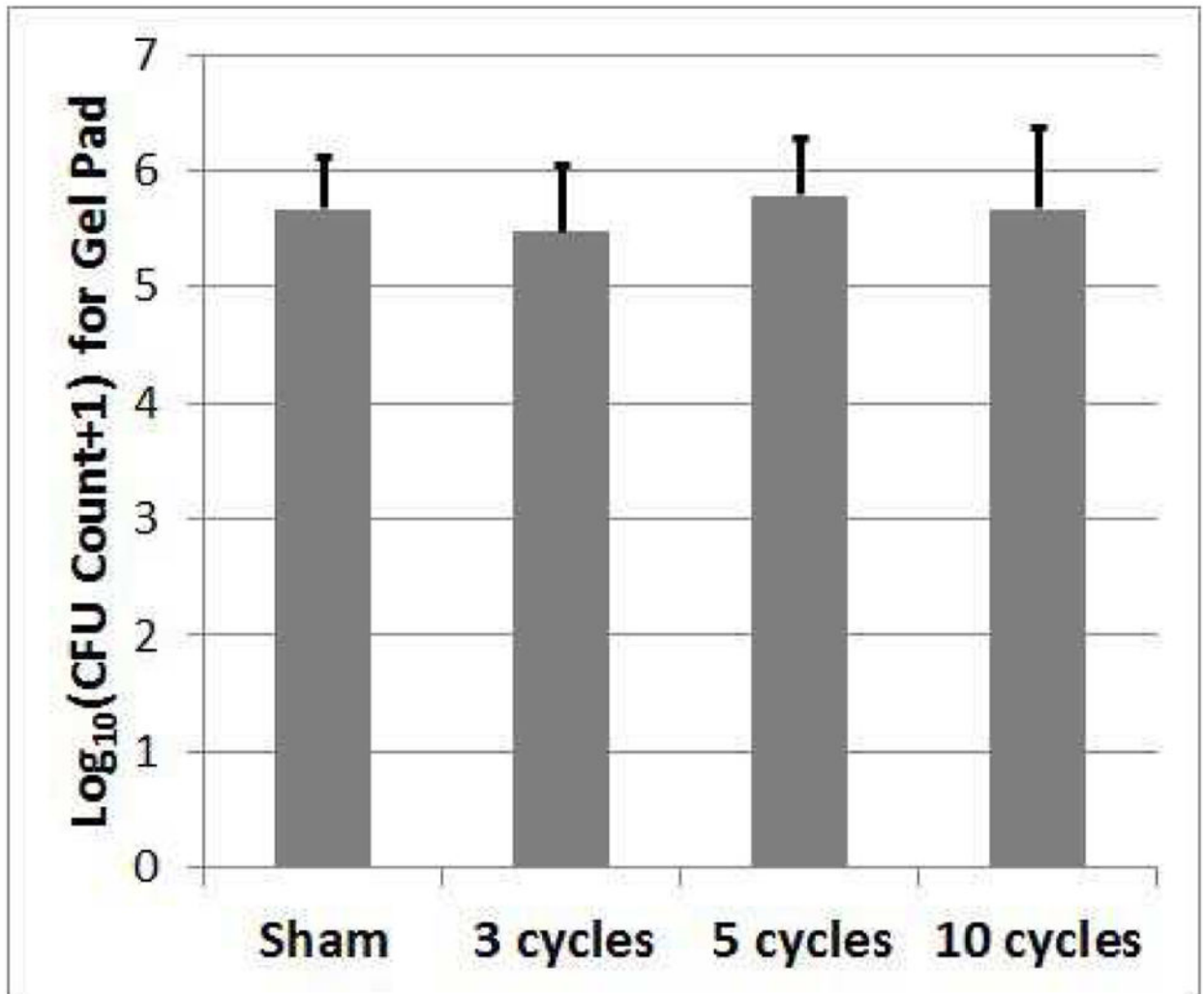


Fig. 5. Count of CFUs surviving on the gel pads following the treatment as a function of the number of cycles in the tone burst used to treat the biofilm on the mesh. The error bars correspond to one standard deviation.

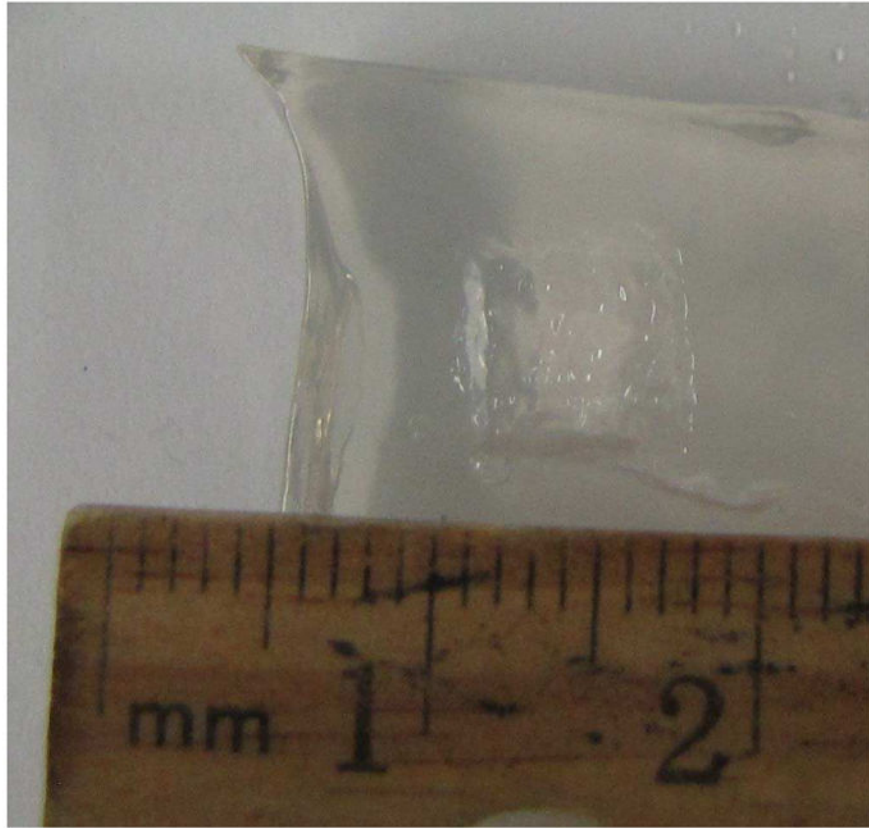


Fig. 6. Example image showing damaged gel sample after rinsing of debris. This example was for a 5-cycle exposure. The square lesion shape with regular pitting in the bottom is visible.

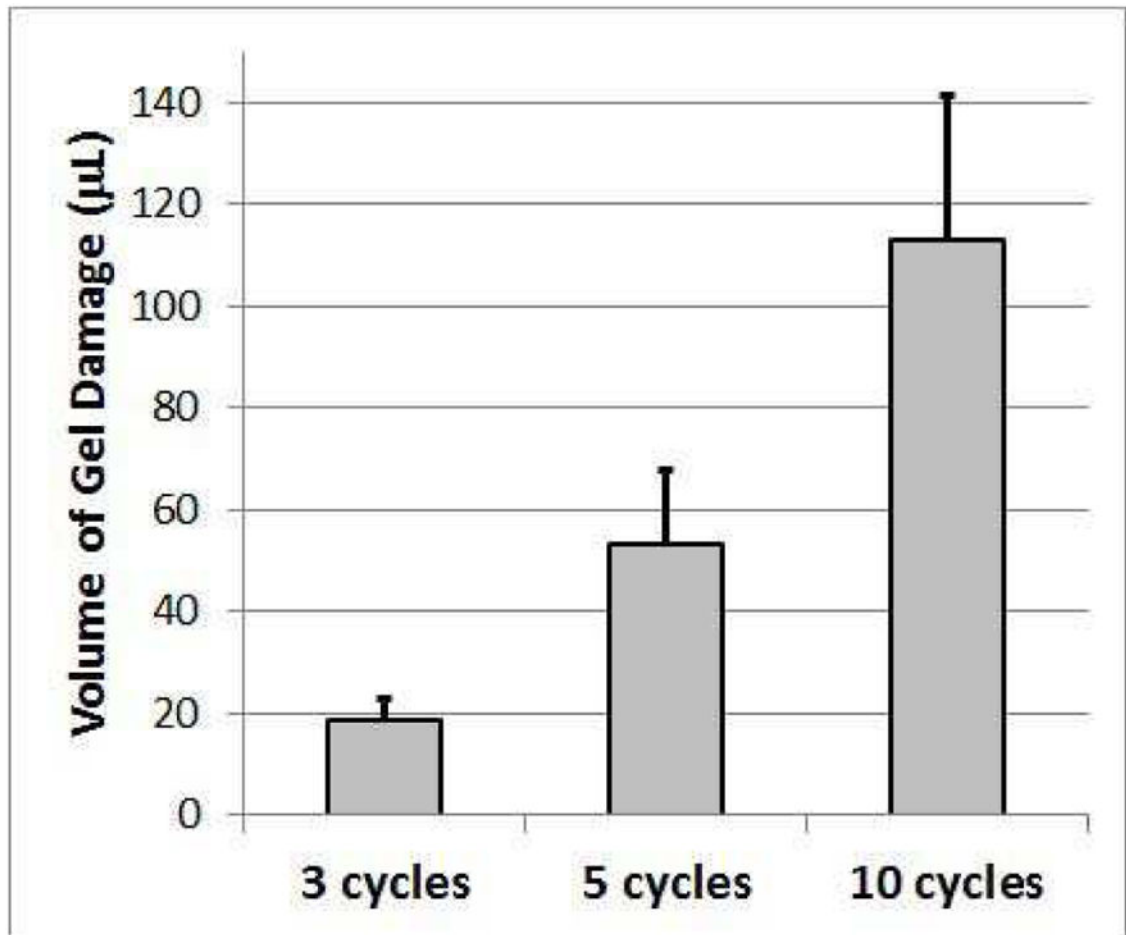


Fig. 7. Volume of gel damaged by treatment as a function of the number of cycles in the tone burst used to treat the biofilm on the mesh. The error bars correspond to one standard deviation.

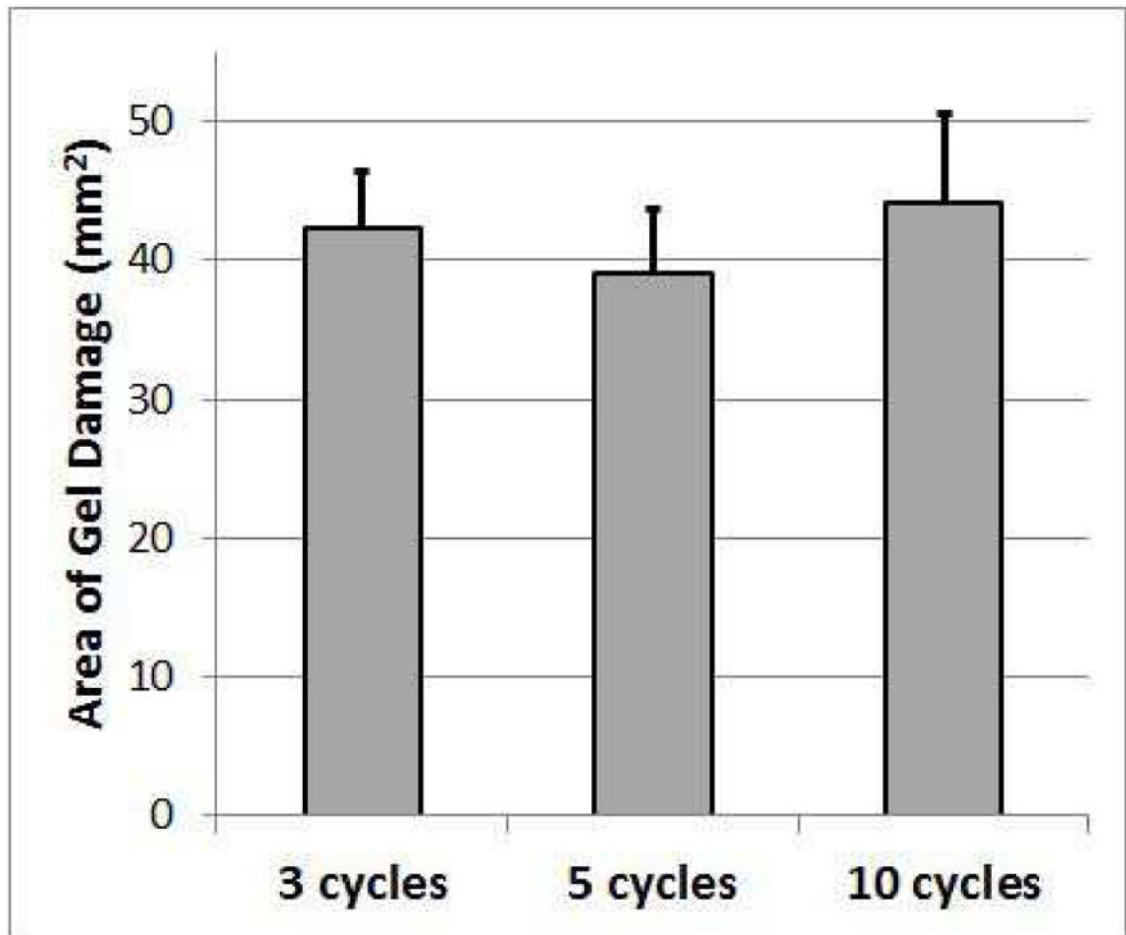


Fig. 8. Cross-Sectional area of gel damaged by treatment as a function of the number of cycles in the tone burst used to treat the biofilm on the mesh. The error bars correspond to one standard deviation.